Clinical Neurophysiology 130 (2019) 2096–2104

Contents lists available at ScienceDirect

Clinical Neurophysiology

journal homepage: www.elsevier.com/locate/clinph

Altered dynamic functional connectivity in weakly-connected state in major depressive disorder

Zhijun Yao [a,1], Jie Shi [a,1], Zhe Zhang [b], Weihao Zheng [b], Tao Hu [c], Yuan Li [d], Yue Yu [a], Zicheng Zhang [a], Yu Fu [a], Ying Zou [a], Wenwen Zhang [e], Xia Wu [f,*], Bin Hu [a,*]

[a] School of Information Science and Engineering, Lanzhou University, Lanzhou, Gansu Province 730000, PR China
[b] College of Biomedical Engineering and Instrument Science, Zhejiang University, Hangzhou, Zhejiang Province 310027, PR China
[c] Graduate School of Informatics, Nagoya University, Nagoya, Aichi 464-8601, Japan
[d] School of Information Science and Engineering, Shandong Normal University, Jinan, Shandong Province 250358, PR China
[e] Department of Radiology, Gansu Provincial Hospital, Lanzhou, Gansu Province 730000, PR China
[f] College of Information Science and Technology, Beijing Normal University, Beijing 100000, PR China

ARTICLE INFO

Article history:
Accepted 14 August 2019
Available online 23 August 2019

Keywords:
Major depressive disorder
Independent component analysis
Dynamic functional connectivity
State-dependent
Resting-state functional magnetic resonance imaging

HIGHLIGHTS

- Dynamic functional connectivity (FC) alterations in major depressive disorder (MDD) were mainly concentrated in weakly-connected state.
- MDD patients exhibited increased mean dwell time and decreased FC in weakly-connected state.
- Dynamics of reduced FC predicted individual differences in depression symptom severity.

ABSTRACT

Objective: Major depressive disorder (MDD) is accompanied by abnormal changes in dynamic functional connectivity (FC) among brain regions. The aim of this study is to investigate whether the abnormalities of dynamic FC in MDD are state-dependent (related to a specific connectivity state).
Methods: We performed time-varying connectivity analysis on resting-state functional magnetic resonance imaging (rs-fMRI) of 49 MDD patients and 54 matched healthy controls (HCs). FC differences between groups in each connectivity state were analyzed and associations between disease severity and dynamics of aberrant FC were explored.
Results: Two distinct connectivity states (i.e., weakly-connected and strongly-connected state) were identified. Compared to HCs, MDD patients were associated with increased mean dwell time and decreased FC between and within subnetworks in the weakly-connected state. Dynamics of reduced FC between cognitive control network and default mode network as well as within cognitive control network predicted individual differences in depression symptom severity.
Conclusions: Our findings suggested that the MDD-caused FC alterations mostly appeared in the weakly-connected state, which might contribute to clinical diagnosis of MDD.
Significance: These findings provide new perspectives for understanding the state-dependent neurophysiological mechanisms in MDD.

1. Introduction

Major depressive disorder (MDD) is one of the leading causes of mortality worldwide characterized by depressed mood, guilt, diminished interests, worthlessness, cognitive impairments, and functional disability (Ferrari et al., 2013; Liu et al., 2010; Zheng et al., 2015). Previous resting-state functional magnetic resonance imaging (rs-fMRI) studies have reported that cognitive

* Corresponding authors at: College of Information Science and Technology, Beijing Normal University, P.O. Box 100000, Beijing, PR China. Fax: +86 10 5880 0056 (X. Wu). School of Information Science and Engineering, Lanzhou University, P.O. Box 730000, Lanzhou, Gansu Province, PR China. Fax: +86 0931 8912 779 (B. Hu).
E-mail addresses: wuxia@bnu.edu.cn (X. Wu), bh@lzu.edu.cn (B. Hu).
[1] These authors contributed to the work equally and should be regarded as co-first authors.

https://doi.org/10.1016/j.clinph.2019.08.009
1388-2457/

impairments in MDD were associated with abnormal functional connectivity (FC) interactions between multiple brain regions and networks (Gong and He, 2015; Mulders et al., 2015). In this respect, the investigation of brain intrinsic FC might facilitate our understanding of the neurophysiological mechanisms underlying the MDD.

In the past decade, great progress has been made in understanding the neural basis of depression via connectivity analysis, and multiple key functional networks have been detected to play an important part in generating different symptoms of depression (Iwabuchi et al., 2014). For example, abnormal FC in resting-state revealed imbalanced communication within individual subnetworks and between distributed subnetworks in patients with MDD (Kaiser et al., 2015; Manoliu et al., 2014). Previous studies also found that the altered FC in MDD cohort in default mode network (DMN, involved in self-referential processing), cognitive control network (CCN, related to attention and working memory), and other cortical or subcortical systems such as visual cortex, cerebellum, and caudate nucleus (Bluhm et al., 2009; Dutta et al., 2014; Mulders et al., 2015). However, these studies were all based on the hypothesis that the FC between brain areas in the whole scanning period was temporally stationary, which omitted the fact that FC might change with the processes that affect cognition, e.g., memorizing and learning, ageing and growth, even during rs-fMRI (Medaglia et al., 2015; Zheng et al., 2018). Dynamically integrated networks could reveal FC variation during a scan process, which might be difficult to achieve in the traditional static network analysis of rs-fMRI.

Recent studies have identified time-varying characteristics of resting-state FC during a scan period using sliding window approach, so called temporal dynamic FC analysis (Allen et al., 2014; Calhoun et al., 2014; Damaraju et al., 2014; Hutchison et al., 2013b; Liu and Duyn, 2013). The derived time-varying patterns across varied windows could reflect the dynamic characteristic of FC, and might be an efficient way to facilitate our understanding of the underlying neurophysiological mechanisms of mental diseases. For example, abnormal dynamic FC was found in varied diseases, such as autism (de Lacy et al., 2017), schizophrenia (Du et al., 2016; Yu et al., 2015), Parkinson's disease (Díez-Cirarda et al., 2018; Kim et al., 2017), minimal hepatic encephalopathy (Chen et al., 2017), mild traumatic brain injury (Vergara et al., 2018), and epilepsy (Liao et al., 2014; Liu et al., 2017). Recently, studies also reported abnormal time-varying FC in patients with MDD. For example, MDD patients showed altered variability of FC in medial prefrontal cortex (Kaiser et al., 2016), and possessed higher global synchronization and temporal stability (Demirtaş et al., 2016). Also, patients with MDD showed altered dynamic FC among different networks and the correlations between personality traits and the brain's dynamic characteristics (Wu et al., 2019; Zhi et al., 2018). In addition, some dynamic FC researches have concentrated on the exploration of FC states, which are defined as reoccurring short-term connectivity patterns across varied windows and subjects (Allen et al., 2014; Damaraju et al., 2014). Weaker and stronger connectivity commonly characterizes FC states, which can be conceptually analogous to electroencephalography (EEG) microstates, short periods during that scalp topography maintains quasi-stable (Lehmann, 1990; Pascual-Marqui et al., 1995). Varied disease-related abnormalities exhibited different sensitivity in FC states. Dynamic changes in weakly-connected state were detected in autism (Yao et al., 2016) and abnormalities of connectivity patterns were more prominent during strongly-connected state in schizophrenia patients (Damaraju et al., 2014), but whether these changes in MDD are state-dependent (related to a specific connectivity state) is not well characterized. The investigation of state-dependent property in MDD might advance our understanding of the disorder. To the best of our knowledge, the present work is the first study to investigate the state-dependent property of the dynamic FC patterns in MDD, which provides new insights into state-dependent mechanisms in MDD.

In the present study, we aim to investigate whether the abnormalities of dynamic FC in MDD are associated with specific state. Group spatial independent component analysis (ICA) and dynamic FC analysis were conducted on rs-fMRI data of 49 patients with MDD and 54 healthy controls (HCs) to extract the whole-brain time-varying functional networks and identify different connectivity states. FC differences between groups in each connectivity state were analyzed using the network-based statistic (NBS) approach. Finally, partial correlation analysis between dynamics of aberrant FC and disease severity was performed.

2. Materials and methods

2.1. Participants

Fifty-nine MDD patients and 65 age-matched and sex-matched HCs participated in the current study. This study was conducted in accordance with the Helsinki Declaration and was approved by the Ethics committee of the Gansu Provincial Hospital. The MDD patients were recruited from the Gansu Provincial Hospital, while the HC subjects were recruited through newspaper advertisements. MDD participants were diagnosed using the Structured Clinical Interview for DSM-IV Axis I Disorders (SCID), and HCs were interviewed using the Structured Clinical Interview for DSM-IV, non-patient edition. Among all the MDD patients, 8 patients (13.56%) were currently medication free, 16 patients (27.12%) were treated with monotherapy (with one of the escitalopram, paroxetine, fluoxetine, deanxit, zoloft, venlafaxine and citalopram), and 35 patients (59.32%) were treated with combination therapy (with two or more of the escitalopram, paroxetine, fluoxetine, deanxit, zoloft, venlafaxine, citalopram, amitriptyline, trazodone, fluvoxoxamine, sulpiride, mirtazapine and maprotiline). All participants provided written informed consent after reading a description of the study procedures.

2.2. Image acquisition

All rs-fMRI data were collected on a 3.0 T Siemens Trio scanner (Siemens, Erlangen, Germany) at Gansu Provincial Hospital. All participants were asked to keep silent, do not move, and close their eyes. Participants were also instructed not to think of anything in particular and do not fall asleep. After the scan, each participant was asked to answer a questionnaire survey to confirm that he or she remained awake and were not thinking during the scanning. The resting-state functional data were acquired using an echo-planar imaging sequence with following parameters: repetition time (TR) = 2000 ms, echo time (TE) = 30 ms, slice thickness = 3.5 mm, slice gap = 0.6 mm, field of view = 220 × 220 mm, in-plane matrix = 64 × 64, flip angle = 90°, and slice number = 33. Finally, 240 functional volumes were collected for each participant.

2.3. Image preprocessing

Imaging data were preprocessed using DPARSFA (Yan and Zang, 2010) based on SPM12 (http://www.fil.ion.ucl.ac.uk/spm). The first 10 volumes for each subject were discarded to allow for equilibration of the magnetic field, resulting in a total of 230 volumes. The remaining volumes underwent slices signal acquisition time correction and were realigned to the first volume for head motion correction. The corrected functional data were spatially normalized to Montreal Neurological Institute (MNI) space with

3 mm × 3 mm × 3 mm resolution and then spatially smoothed with a 8-mm full-width at half-maximum (FWHM) Gaussian kernel. Notably, participants with the maximum translation > 2 mm, rotation > 2° (4 MDD patients and 1 HCs), or frame-wise displacements (FD) > 1 mm (6 MDD patients and 10 HCs) were excluded to minimize the potential influence of head motion. According to the exclusion criteria, the analyses were carried out with 49 MDD patients and 54 HCs. The mean FD was calculated for each participant (<0.5 mm) based on the realignment parameters and there was no significant difference between two groups ($p = 0.74$).

2.4. Group ICA

A data-driven technique of group spatial ICA was performed via Group ICA of fMRI Toolbox (GIFT) (Calhoun et al., 2001) (http://mialab.mrn.org/software/gift/) on the preprocessed rs-fMRI data, which decomposed the data into spatial independent components (ICs). Specifically, 150 principal components (PCs) for subject-specific data were obtained by the principal component analysis (PCA). In the group-level data reduction, group data formed by concatenating subjects reduced data were further decomposed into 100 PCs using PCA. The Infomax ICA algorithm (Bell and Sejnowski, 1995) was then used to obtain 100 ICs. The reliability of the decomposition was evaluated by repeating the algorithm 20 times in ICASSO (Himberg et al., 2004). Subject-specific spatial maps (SMs) and time-courses (TCs) for each IC were acquired using the GICA back reconstruction algorithm. In the present study, we identified 49 ICs based on the criteria by (Allen et al., 2011; Allen et al., 2014) : (1) peak coordinates of spatial maps located primarily in grey matter; (2) low spatial overlap with known vascular, ventricular, motion, and susceptibility artifacts; (3) TCs dominated by low frequency fluctuations; and (4) TCs characterized by a high dynamic range (a range difference between the minimum and maximum power frequencies). Based on anatomy and prior knowledge of their function (Allen et al., 2014, Damaraju et al., 2014; Rashid et al., 2014), 49 ICs were categorized into seven subnetworks for further analysis. The seven subnetworks were subcortical (SC), auditory (AU), visual (VIS), sensorimotor (SM), cognitive control (CC), default mode (DM), and cerebellar (CB) networks (see Fig. 1A; Supplementary Table S1).

We performed post processing on TCs of 49 ICs. Briefly, linear, quadratic and cubic trends of time courses were removed, and six realignment parameters and their temporal derivatives were regressed out. Then, the regressed time serials were despiked by 3DDESPIKE to detect and remove the outliers, and filtered with the high cutoff frequency of 0.15 Hz (Allen et al., 2014). Pair-wise Pearson's correlations were computed using the post processed TCs between ICs over the entire scan to obtain the static FC matrix, which was then converted to z-value via Fisher's z-transformation (Kim et al., 2017) (see Fig. 1B).

2.5. Dynamic FC state analysis

Dynamic FC was calculated based on a sliding window approach using GIFT toolbox. We used a tapered window created by convolving a rectangle (width = 22 TRs) with a Gaussian ($\sigma = 3$ TRs). By sliding the time window in steps of 1TR along the 230-TRs length scan, we obtained 208 consecutive windows across the entire scan. For each window, 49 × 49 pair-wise covariance matrix was calculated by the regularized inverse covariance matrix (Varoquaux et al., 2010) using the graphical LASSO framework (Friedman et al., 2008). The regularization parameter lambda was optimized for each subject by using a cross-validation framework. Values in the resulting dynamic FC matrices were Fisher-Z transformed and then residualized with age and gender. Therefore, 208 FC matrices were obtained from each participant, which represented the time-varying FC during the whole scan time. To measure FC fluctuation, we defined the variance of FC across the entire scan (208 windows) as FC dynamic.

After sliding windows step, k-means clustering method was applied on all FC matrices of windows to estimate reoccurring FC states in all participants. The similarity between each FC matrix was estimated by using the L1 (Manhattan) distance, which is an effective method for high dimensional data (Aggarwal et al., 2001). The K-means clustering method was first repeated 100 times to obtain the unbiased initial cluster centroids, and then were used to regroup all window FC matrices into several clusters based on the similarity measurement. Here, we evaluated the optimal number of clusters by using the cluster number validity analysis (gap statistic and silhouette) on the subsampling windows of

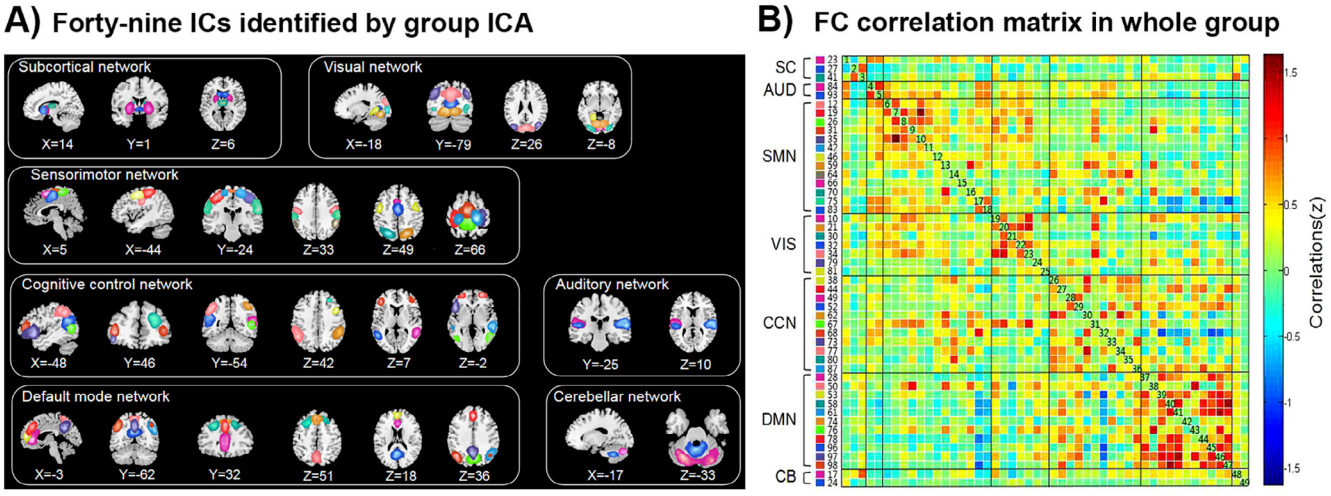

Fig. 1. SMs from the 49 ICs and static functional connectivity network. (A) Forty-nine ICs divided in 7 functional networks. **(B)** The static FC between ICs in the whole sample. Index numbers of ICs are written on the left side of the matrix, along with a color-coded legend, which corresponds to the overlaid colors of the spatial maps in **(A)**. The colorbar represents the z value of the correlations; Red color represents positive correlations and blue color represents negative correlations. Abbreviation: SMs, spatial maps; IC, independent component; ICA, independent component analysis; FC, functional connectivity; SC, subcortical network; AUD, auditory network; VIS, visual network; SMN, sensorimotor network; CCN, cognitive control network; DMN, default mode network; CB, cerebellar network. (For interpretation of the references to colour in this figure legend, the reader is referred to the web version of this article.)

all subjects varying k from 2 to 10 (Kim et al., 2017; Rousseeuw, 1987; Tibshirani et al., 2001). The effectiveness of the states in the MDD and HCs was determined by the span of states in window numbers. In this study, a state was considered reliable only when it covered at least 10 windows.

We examined the temporal properties of dynamic FC states derived from each participant's state vector. Specifically, we assessed two measures in subjects, including: (1) mean dwell time in each state, measured as the average number of consecutive windows in a certain state before changing to the other state; (2) number of transitions, measured as the number of times that the state switched from one to the other. The between-group differences of these metrics were assessed by using Mann-Whitney U-test in the Statistical Package for Social Science (SPSS) (IBM SPSS Statistics 21).

A participant median was estimated for each cluster division from the participant windows that were assigned to that cluster, representing the connectivity pattern of each participant in that state (Damaraju et al., 2014). The between-group differences of FC in each state were analyzed by comparing medians in participants of different states via NBS approach (Liu et al., 2017; Zalesky et al., 2010). Note that not all participants had dynamic FC windows assigned to each state, in which case the statistical analysis on a given state was only performed for participants who had windows in that cluster. Here, nodes were defined as ICs whose locations were specified with the peak coordinates of ICs, and the edges were represented with the correlation values of FC matrix (Díez-Cirarda et al., 2018). A t-test contrasting the two groups was computed for each pair-wise connection, based on the values stored in each subject's connectivity matrix. The connections with a t-statistic exceeding the primary t-statistic threshold were admitted to a set of supra-threshold connections, within which any connected components and their size (number of connections) could then be determined. Permutation testing was used to ascribe a p-value controlled for the family-wise error rate (FWE) to each connected component based on its size. For each permutation, the size of the largest component was recorded to generate an empirical estimate of the null distribution. A corrected p-value was calculated for each component utilizing the null distribution of maximal connected component size (Zalesky et al., 2010; Zalesky et al., 2011). For the NBS, we performed the two dimension comparison of MDD and HCs. The contrasts were set as "MDD > controls" and "MDD < controls". The permutations were repeated for 5000 times and the primary t-statistic threshold was set as $t > 2.7$. The threshold of multiple comparisons was set as corrected $p < 0.05$. We also computed the partial correlation between the dynamics of altered FC and HAMD scores in MDD patients, by controlling for age and gender.

3. Results

3.1. Demographic characteristics

Table 1 demonstrated all statistical differences on the demographical and neuropsychological performances between the MDD and HC groups. We did not detect significant differences in the age, gender, and mean FD variables ($p = 0.355$, $p = 0.382$, and $p = 0.74$). There were significant differences in the HAMA ($p < 0.001$) and HAMD ($p < 0.001$) scores between the two groups.

3.2. Clustering analysis

The gap statistic presented little discrimination for each k value, while the silhouette statistic showed highest silhouette coefficient at k = 2. Combining the gap statistic and silhouette, the optimal number of clusters was determined to be two (k = 2) (see Supplementary Fig. S1). Based on the k-means clustering method, two reoccurring state patterns were identified during the rs-fMRI acquisition and across the whole sample. As illustrated in Fig. 2A, state 1 occurred more frequently (84%) which was characterized by the presence of weaker connectivity, whereas state 2 occurred less frequently (16%) which was characterized by stronger connectivity. The strongest 5% connections of each state were kept for better visualization to display the distinct pattern of two states (see Fig. 2B). Generally, ICs of the brain could be divided into low-level perceptual network (SMN, VIS and AUD) and high-level cognitive network (DMN and CCN). State 1 (the weakly-connected state) exhibited high integration in the cognitive network, while state 2 (the strongly-connected state) showed high connectedness of perceptual network. Specifically, state 1 showed positive correlations located mainly within DMN/CCN and between these two networks, and negative correlations were mainly found between CCN and DMN (and between SMN and DMN). In contrast, state 2 exhibited distributed positive connections mainly within and between perceptual networks (i.e., AUD, SMN and VIS) and several connections between CCN and SMN, VIS.

Table 1
Demographics and clinical characteristics of the participants.

Characteristics	MDD (n = 49) (Mean ± SD)	HCs (n = 54) (Mean ± SD)	P-value
Age (years)	33.14 ± 11.39	35.33 ± 12.45	0.355[a]
Gender (males/females)	26/23	24/30	0.382[b]
Handedness (right/left)	49/0	54/0	–
HAMD	17.47 ± 5.95	0.37 ± 0.71	<0.001[a]
HAMA	17.16 ± 6.91	0.61 ± 0.88	<0.001[a]
Illness Duration (years)	7.35 ± 8.33	–	–
Mean FD	0.129 ± 0.07	0.134 ± 0.05	0.74[a]

Abbreviations: HAMA, Hamilton Anxiety Scale; HAMD, Hamilton Depression Rating Scale; FD, frame-wise displacement; MDD, major depressive disorder; HCs, healthy controls; SD, standard deviation.
[a] Two-sample t-test.
[b] Chi-square test.

With respect to the dwell time in states, MDD patients exhibited significantly ($p = 0.041$, Mann-Whitney U-test) longer mean dwell time in state 1 (the weakly-connected state) (see Fig. 3A). In addition, the difference in transition times between the two cohorts was marginally significant ($p = 0.070$, Mann-Whitney U-test) (see Fig. 3B).

3.3. Dynamic FC differences

Compared to the HCs, MDD patients showed reduced connections between and within subnetworks in weakly-connected state (corrected $p < 0.05$) (see Table 2, Fig. 4A), which were mostly found between CCN and DMN. Other reductions were the connections between SC and CCN, SC and DMN, SMN and CCN, VIS and DMN, as well as the connections within CCN. There was no significant difference of FC in strongly-connected state between MDD patients and HCs. Furthermore, the dynamics of altered FC in CCN-DMN and CCN-CCN had significant negative correlation with the symptom severity. Specifically, the dynamics of connections that link middle temporal gyrus (MTG, IC49) with both medial frontal gyrus (medFG, IC74) and inferior frontal gyrus (orbital) (ORBinf, IC73) could predict the severity of depressive symptoms in MDD patients, with $r = -0.41$ ($p = 0.004$, uncorrected) and $r = -0.30$ ($p = 0.044$, uncorrected), respectively (see Fig. 4B, C, D).

4. Discussion

Recently, many studies began to capitalize on the wealth of information hiding behind the temporal features, such as

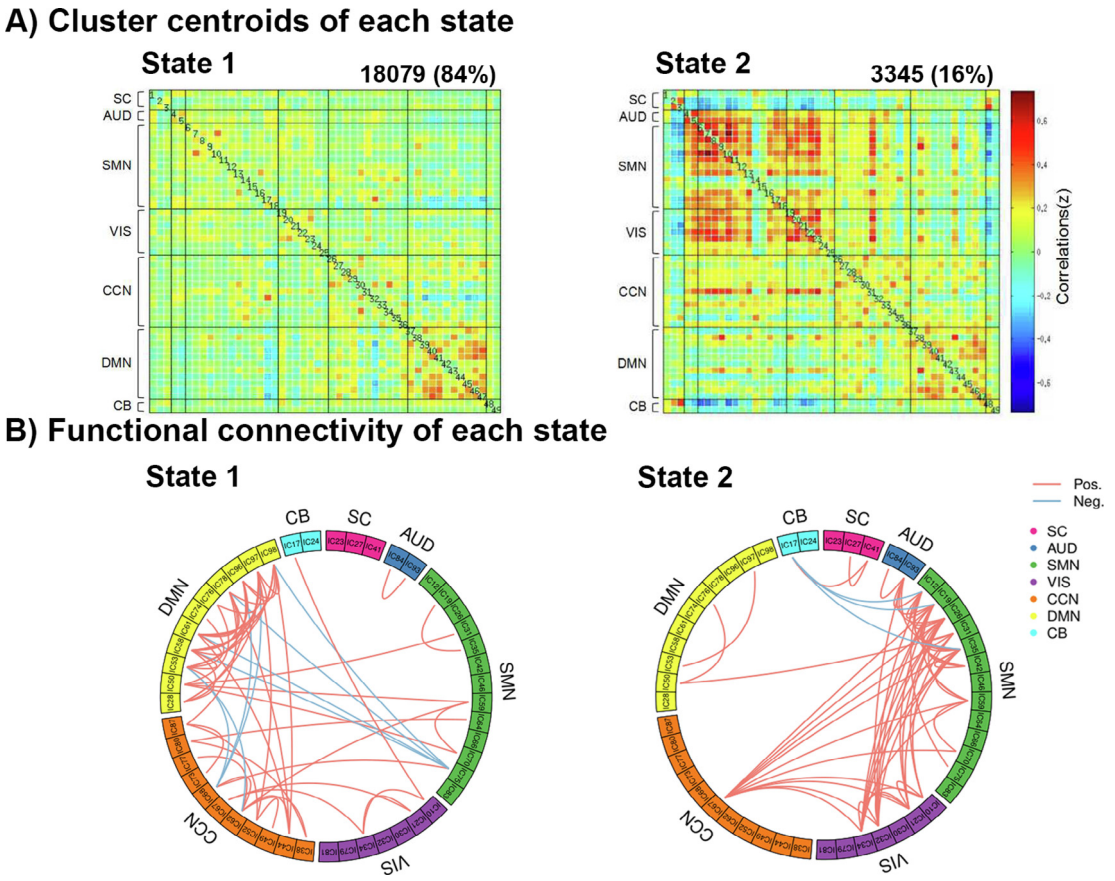

Fig. 2. Results of the clustering analysis in the whole sample. (A) Cluster centroids for each state. The total number of occurrences and percentage of total occurrences are listed for each state. The colorbar represents the z value of the correlations; Red color represents positive correlations and blue color represents negative correlations. **(B)** The strongest 5% connections of each state. Each rectangle on the circumference of the big circle represents each IC, and each rectangle color represents one of the seven networks (i.e., SC, AUD, SMN, VIS, CCN, DMN and CB). The lines connecting the rectangle pairs represent the connections between the corresponding two ICs. The red lines represent positive correlations and blue lines represent negative correlations. Abbreviation: SC, subcortical network; AUD, auditory network; VIS, visual network; SMN, sensorimotor network; CCN, cognitive control network; DMN, default mode network; CB, cerebellar network. (For interpretation of the references to colour in this figure legend, the reader is referred to the web version of this article.)

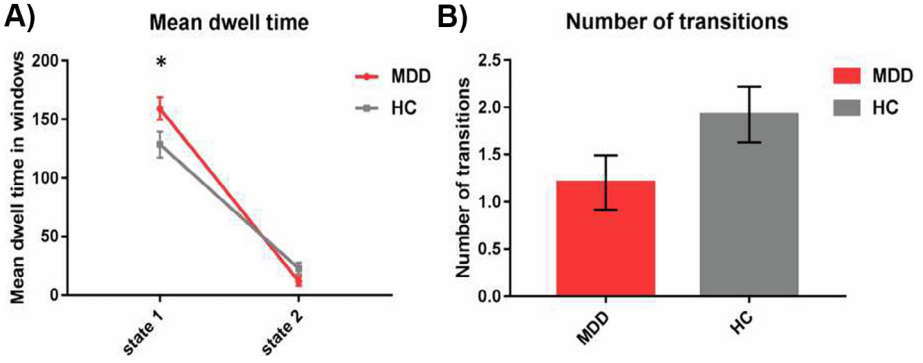

Fig. 3. Temporal properties differences between groups. Asterisks indicate significant differences between groups. Error bars represent the standard error. Abbreviation: MDD, major depressive disorder; HCs, healthy controls.

time-varying FC and the derived dynamic FC metrics, which might index changes in macroscopic neural activity patterns underlying critical aspects of cognition and behavior (Hutchison et al., 2013a). Our results showed that the altered connectivity of MDD patients exhibited evident state-dependent property, in which the abnormalities were largely related to the weakly-connected state. These findings provide new insights into understanding of the neurophysiological mechanisms underlying MDD.

In the present study, two different connectivity states, including a weakly-connected state and a strongly-connected state, were identified across the whole sample. The weakly-connected state was characterized by positive correlations located mainly within DMN and CCN and between these two networks, and the negative correlations were mainly between CCN and DMN (and between SMN and DMN). DMN and CCN are known as high-level cognitive networks that play critical roles in the pathophysiology of MDD

Table 2
FC reductions in weakly-connected state in MDD compared to HCs.

FC reductions	Test statistic (t values)	
CCN-DMN		
Middle temporal gyrus_BA39L	Anterior cingulate cortex_BA32L	3.88
Middle temporal gyrus_BA22R	Anterior cingulate cortex_BA32L	3.12
Inferior frontal gyrus (orbital) _BA47L	Anterior cingulate cortex_BA32L	3.44
Middle temporal gyrus_BA21R	Anterior cingulate cortex_BA32L	2.95
Middle temporal gyrus_BA22R	Medial frontal gyrus_BA8R	2.74
SC-CCN		
Caudate nucleus L	Middle frontal gyrus (orbital) _BA10R	3.27
Thalamus L	Middle frontal gyrus (orbital) _BA10R	3.79
Thalamus L	Inferior parietal lobule_BA40L	2.96
SC-DMN		
Thalamus L	Precuneus_BA7R	2.89
Caudate nucleus L	Medial frontal gyrus_BA8R	2.76
CCN-CCN		
Middle temporal gyrus _BA22R	Inferior frontal gyrus (orbital) _BA47L	2.73
Inferior frontal gyrus (triangular) _BA9R	Inferior parietal lobule_BA40L	3.05
SMN-CCN		
Supplementary motor area_BA6L	Middle frontal gyrus (orbital) _BA10R	3.02
VIS-DMN		
Calcarine _BA18	Precuneus_BA7R	2.96

Abbreviations: FC, functional connectivity; MDD, major depressive disorder; HCs, healthy controls; SC, subcortical network; VIS, visual network; SMN, sensorimotor network; CCN, cognitive control network; DMN, default mode network; BA, brodmann area; R, right; L, left.

(Hamilton et al., 2013; Manoliu et al., 2014; Menon, 2011). The high integration of DMN and CCN in weakly-connected state suggested that the weakly-connected state might be more related to the high-level cognitive functions (e.g., monitoring the internal mental landscape, attentional capture, and allocate cognitive resources) (Gusnard et al., 2001; Menon, 2011; Mulders et al., 2015; Qin and Northoff, 2011). Specifically, DMN has been reported to be associated with specific MDD clinical characteristics like exaggerated self-focus and depressive maladaptive ruminations (Berman et al., 2010; Demirtaş et al., 2016; Hamilton et al., 2011); CCN is related to attention allocation, working memory and cognitive inhibition, which enables participants to flexibly adapt information processing to changing situational demands (Carter and Van Veen, 2007; Miller and Cohen, 2001). In addition, CCN is responsible for regulating DMN activity during cognitive processing (Chen et al., 2013; Dong et al., 2019). In contrast, the strongly-connected state exhibited distributed positive connections mainly within and between the perceptual network (i.e., SMN, VIS and AUD). The perceptual network is related to sensory perception and motor process which play a central role in information transfer with external environment (Liu et al., 2017). Moreover, the connections between CCN and SMN, VIS may reflect the top-down control mechanism that allowed CCN to modulate motion and perception, which is essential to the switch of effective cognitive processing to action (Christopher et al., 2015; Gazzaley et al., 2005a; Gazzaley et al., 2005b). The main aspects of depressive symptomatology include rumination, emotional disinhibition and impaired cognitive control, which are related to the high-level functioning systems (Brakowski et al., 2017; Hamilton et al., 2013). Therefore, we speculated the connectivity abnormalities in

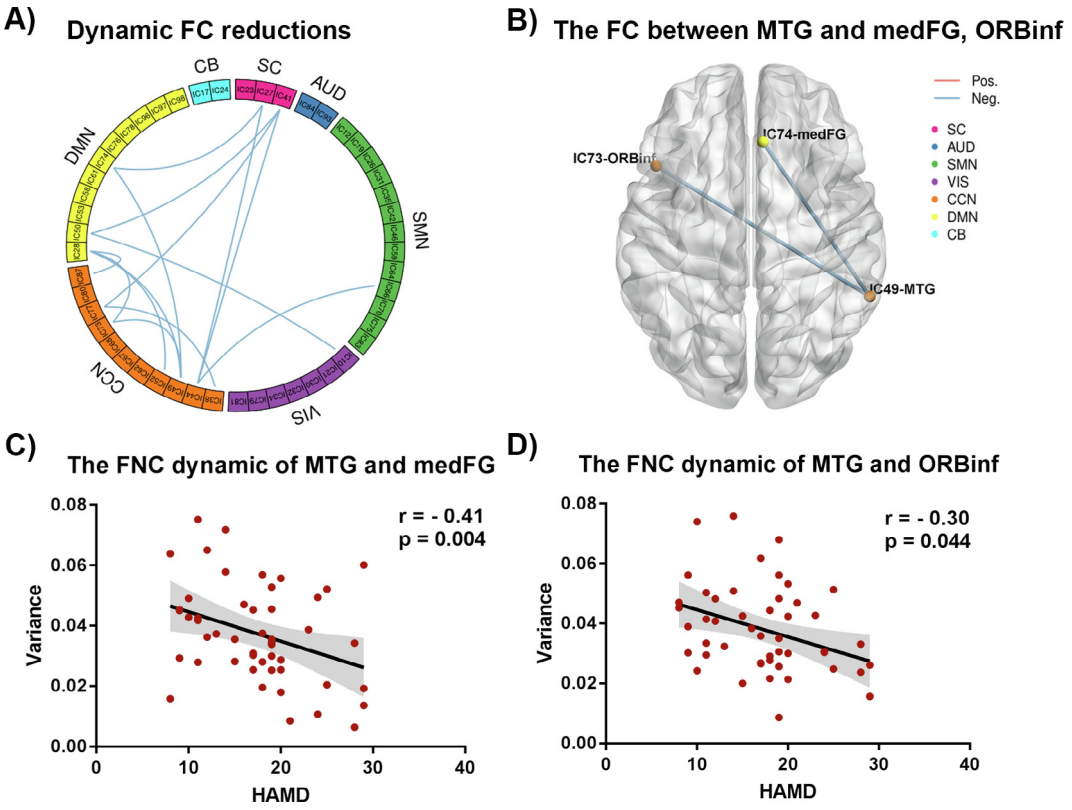

Fig. 4. Results of dynamic FC analysis. (A) FC reductions in weakly-connected state in MDD compared to HCs. **(B)** The FC which dynamics significantly correlated with HAMD. **(C), (D)** Significant correlation between the FNC dynamics and HAMD. Abbreviation: IC, independent component; FNC, functional network connectivity; HAMD, Hamilton Depression Rating Scale; MTG, middle temporal gyrus; medFG, medial frontal gyrus; ORBinf, inferior frontal gyrus (orbital); SC, subcortical network; AUD, auditory network; VIS, visual network; SMN, sensorimotor network; CCN, cognitive control network; DMN, default mode network; CB, cerebellar network.

MDD patients might be more related to the weakly-connected state.

The significant FC changes in weakly-connected state among MDD patients supported our speculation. Abnormal dynamic FC in MDD was observed primarily in CCN, DMN, and SC, which were related to emotion regulation and cognitive function (Kaiser et al., 2015; Kober et al., 2008; Mulders et al., 2015). Specifically, significant reduction of connections within CCN and between subnetworks were found in weakly-connected state. Previous studies in patients with depression also showed reduced FC between anterior cingulate cortex (ACC) and MTG (in this study: CCN-DMN) (Lui et al., 2011), decreased FC between caudate and middle orbitofrontal cortex (in this study: SC-CCN) (Ma et al., 2012), decreased connectivity between thalamus and posterior cingulate cortex/precuneus (in this study: SC-DMN) (Guo et al., 2013a), reduced connectivity between the orbitofrontal cortex and the middle temporal cortex in an explicit task (in this study: CCN-CCN) (Frodl et al., 2010), and decreased connectivity between calcarine and precuneus (in this study: VIS-DMN) (Guo et al., 2013b). Interestingly, the decreased FC in weakly-connected state was found mostly between CCN and DMN. Previous findings showed abnormal FC in DMN (Greicius et al., 2007; Zhu et al., 2012; Zhu et al., 2017) and CCN (Alexopoulos et al., 2012; Sexton et al., 2012; Ye et al., 2012), as well as decreased communication between the two subnetworks in depression patients (de Kwaasteniet et al., 2015). Since DMN is associated with self-referential properties (Sheline et al., 2009) and CCN is involved in cognitive processing (Corbetta and Shulman, 2002), the alteration in DMN-CCN communication may underlie difficulty in switching from a "default-state" to an "executive state" (Hamilton et al., 2013; Mulders et al., 2015). Moreover, decreased connectivity within DMN and CCN may suggest that negative self-referential dominate over cognitive processing, which is highly related to the clinical behavior of MDD patients (Mulders et al., 2015). In addition, studies reported decreased FC that connected anterior cingulate cortex (ACC) with MTG and inferior frontal gyrus (IFG) in patients with depression compared to the HCs (Cullen et al., 2009; Lui et al., 2011). Consistent with these findings, we found significant reduction in connectivity linking ACC with both MTG and ORBinf in weakly-connected state among patients with MDD. These connectivity changes might be relevant to dramatic morphological atrophy of ACC (Abe et al., 2010; Du et al., 2012) and MTG (Ma et al., 2012) in patients with MDD, and the altered connectivity between MTG and DMN might contribute to the negative thoughts and negative emotional experience in depression (Ma et al., 2012). The present study also showed decreased FC between CCN and DMN located in MTG and medFG in MDD patients. The medFG, a marker of vulnerability for depression, is central to self-referential processing and emotion regulation (Lemogne et al., 2009), while MTG is located in the extended dorsal attention system and is involved in cued attention and working memory (Corbetta and Shulman, 2002; Fox et al., 2006). The decreased connectivity in CCN and DMN might suggest abnormalities in regulation of emotion of MDD patients. Additionally, the FC changes in weakly-connected state indicated that abnormal dynamic FC underlies the negative, dysregulated thinking mode that characterizes depression (Kaiser et al., 2016).

Recent dynamic FC study reported that MDD patients had significantly longer mean dwell time in the weakly-connected state, which was associated with self-focused thinking (Zhi et al., 2018). In line with the previous finding, our results also showed MDD patients spend significantly longer time in the weakly-connected state, which might because of more investment on self-focused rumination during the resting-state (Berman et al., 2014; Marusak et al., 2017). Similar changes were also reported in other psychiatric disorders, such as autism (Yao et al., 2016) and schizophrenia (Damaraju et al., 2014). In addition, the state transition times exhibited marginally significant difference across two groups. The less transition times in MDD patients might indicate that MDD exhibited more stable network dynamic pattern in the entire scan process.

Other findings also supported our speculation that MDD might be more sensitive to the weakly-connected state. HAMD is a valid and easily applicable measure of evaluating depression severity. The high accuracy and specificity of the HAMD make this instrument more suitable for diagnostic purposes (Aben et al., 2002). We found that the dynamics of reduced FC within CCN (MTG-ORBinf), and between CCN and DMN (MTG-medFG), had significant negative correlations with the HAMD scores in weakly-connected state. It should be noticed that the reduced FC here both connected to the MTG, which is related with perception of intentional behavior, the recall of memories and personal experiences. In addition, MTG mediates the ability to explain and predict individual behavior by attributing to independent mental states (e.g., beliefs, emotions, and intentions), which indicates that this region regulates semantic, emotion, and cognition (Gallagher and Frith, 2003; Guo et al., 2017). Accordingly, abnormal MTG-related FC might cause emotional dysregulation. Previous study reported that the DMN and CCN might represent important neural substrates of MDD (Ye et al., 2015). Moreover, reduced mean connectivity within the entire CCN was stable and reliable over time and could represent a biomarker for trait phenotypes of depression risk (Stange et al., 2017). Compatible with the previous studies, the results of negative correlations between FC dynamics and HAMD scores indicated that more stable dynamics of FC between MTG and medFG, ORBinf in weakly-connected state, the patients would have more severe depressive symptoms. The significant correlations provided additional insights in the context of a dynamic perspective as dynamics of FC in weakly-connected state implicated the symptom severity in MDD, and contributed to the identification of efficient biomarkers and the potential aid in clinical diagnosis of MDD.

Several limitations should be addressed in the future work. First, most MDD patients were medicated with different antidepressant medications such as citalopram, zoloft, fluoxetine, fluvoxoxamine, amitriptyline. A large number of studies have reported the effects of antidepressant medication on rs-fMRI data, which have been examined by FC (Li et al., 2013), amplitude of low-frequency fluctuations (Wang Li-Juan et al., 2014), degree centrality (Shen et al., 2015), regional homogeneity (Wang L et al., 2014), etc. For example, Van Wingen et al. explored the effects of duloxetine treatment in healthy subjects revealing the reduction of resting-state FC within the DMN and the task positive network, which may contribute to their antidepressant effects in depression (Van Wingen et al., 2014). Our findings might be confounded by the use of antidepressant medications, which might act to improve depressed patients' abnormalities in emotional reactivity and deficits in emotional regulation (Ma, 2015). In future studies, it would be important to assess the effects of antidepressant medications on dynamic function. Second, an empirically validated fixed sliding window of 22 TR (44 s) was selected in sliding window analysis same to (Damaraju et al., 2014; Zhang et al., 2018). The selection of sliding window size is still inconclusive and may impact the evaluation of dynamic FC. Connectivity changes using separate windows of various windows lengths will be evaluated in the future study. Third, the sample sizes included in the current study is relatively small, the replication study with more participants needs to be performed in the future to verify our findings. Forth, determining reasonable connectivity states is a critical and controversial issue in the field of dynamic FC. It would be beneficial to develop and improve more effective methods for the identification of FC states, providing more reference for clinical diagnosis. Finally, the evolution of dynamic FC during progression of MDD and following various therapies cannot be determined in this study. Thus,

future longitudinal studies are necessary to explore potential altered dynamic FC as a clinical biomarker.

5. Conclusion

In summary, the present study revealed that the abnormalities of FC in MDD patients were mainly concentrated in weakly-connected state. MDD patients spend more time and exhibited decreased FC between and within subnetworks in weakly-connected state. Moreover, lower variability in reduced FC related to the disease severity also implied that the dynamic changes of FC might serve as efficient biomarkers for potential aid in clinical diagnosis, and weakly-connected state might play a key role in detecting symptom severity in MDD. These findings provide new perspectives for understanding the state-dependent neurophysiological mechanisms in MDD.

Declaration of Competing Interest

The authors declare no potential conflict of interest.

Acknowledgments

The authors gratefully acknowledge Gansu Provincial Hospital for the contributions in MRI data acquisition. We are also grateful to all participants in this study. This study was supported by the National Basic Research Program of China (973 Program) (No. 2014CB744600); the National Natural Science Foundation of China (Grant No. 61632014, No. 61627808, No. 61210010); the Program of Beijing Municipal Science & Technology Commission (No. Z171100000117005); the National Key Research and Development Program of China (No. 2016YFC1307203); and the Fundamental Research Funds for the Central Universities (lzujbky-2017-kb08).

Appendix A. Supplementary material

Supplementary data to this article can be found online at https://doi.org/10.1016/j.clinph.2019.08.009.

References

Abe O, Yamasue H, Kasai K, Yamada H, Aoki S, Inoue H, et al. Voxel-based analyses of gray/white matter volume and diffusion tensor data in major depression. Psychiat Res: Neuroimag 2010;181(1):64–70.
Aben I, Verhey F, Lousberg R, Lodder J, Honig A. Validity of the beck depression inventory, hospital anxiety and depression scale, SCL-90, and hamilton depression rating scale as screening instruments for depression in stroke patients. Psychosomatics 2002;43(5):386–93.
Aggarwal CC, Hinneburg A, Keim DA. On the surprising behavior of distance metrics in high dimensional space. International conference on database theory. Springer; 2001. p. 420–34.
Alexopoulos GS, Hoptman MJ, Kanellopoulos D, Murphy CF, Lim KO, Gunning FM. Functional connectivity in the cognitive control network and the default mode network in late-life depression. J Affect Disord 2012;139(1):56–65.
Allen EA, Erhardt EB, Damaraju E, Gruner W, Segall JM, Silva RF, et al. A baseline for the multivariate comparison of resting-state networks. Front Syst Neurosci 2011;5:2.
Allen EA, Eswar D, Plis SM, Erhardt EB, Tom E, Calhoun VD. Tracking whole-brain connectivity dynamics in the resting state. Cereb Cortex 2014;24(3):663–76.
Bell AJ, Sejnowski TJ. An information-maximization approach to blind separation and blind deconvolution. Neural Comput 1995;7(6):1129–59.
Berman MG, Misic B, Buschkuehl M, Kross E, Deldin PJ, Peltier S, et al. Does resting-state connectivity reflect depressive rumination? A tale of two analyses. Neuroimage 2014;103:267–79.
Berman MG, Peltier S, Nee DE, Kross E, Deldin PJ, Jonides J. Depression, rumination and the default network. Social Cognit Affect Neurosci 2010;6(5):548–55.
Bluhm R, Williamson P, Lanius R, Théberge J, Densmore M, Bartha R, et al. Resting state default-mode network connectivity in early depression using a seed region-of-interest analysis: Decreased connectivity with caudate nucleus. Psychiatry Clin Neurosci 2009;63(6):754–61.
Brakowski J, Spinelli S, Dörig N, Bosch OG, Manoliu A, Holtforth MG, et al. Resting state brain network function in major depression–depression symptomatology, antidepressant treatment effects, future research. J Psychiatr Res 2017;92:147–59.
Calhoun VD, Adali T, Pearlson GD, Pekar JJ. A method for making group inferences from functional MRI data using independent component analysis. Hum Brain Mapp 2001;14(3):140–51.
Calhoun VD, Miller R, Pearlson G, Adalı T. The chronnectome: time-varying connectivity networks as the next frontier in fMRI data discovery. Neuron 2014;84(2):262–74.
Carter CS, Van Veen V. Anterior cingulate cortex and conflict detection: an update of theory and data. Cognit Affect Behav Neurosc 2007;7(4):367–79.
Chen AC, Oathes DJ, Chang C, Bradley T, Zhou Z-W, Williams LM, et al. Causal interactions between fronto-parietal central executive and default-mode networks in humans. Proc Natl Acad Sci 2013;110(49):19944–9.
Chen H-J, Lin H-L, Chen Q-F, Liu P-F. Altered dynamic functional connectivity in the default mode network in patients with cirrhosis and minimal hepatic encephalopathy. Neuroradiology 2017;59(9):905–14.
Christopher L, Duff-Canning S, Koshimori Y, Segura B, Boileau I, Chen R, et al. Salience network and parahippocampal dopamine dysfunction in memory-impaired Parkinson disease. Ann Neurol 2015;77(2):269–80.
Corbetta M, Shulman GL. Control of goal-directed and stimulus-driven attention in the brain. Nat Rev Neurosci 2002;3(3):201.
Cullen KR, Gee DG, Klimes-Dougan B, Gabbay V, Hulvershorn L, Mueller BA, et al. A preliminary study of functional connectivity in comorbid adolescent depression. Neurosci Lett 2009;460(3):227–31.
Damaraju E, Allen EA, Belger A, Ford JM, McEwen S, Mathalon D, et al. Dynamic functional connectivity analysis reveals transient states of dysconnectivity in schizophrenia. NeuroImage: Clin 2014;5:298–308.
de Kwaasteniet BP, Rive MM, Ruhé HG, Schene AH, Veltman DJ, Fellinger L, et al. Decreased resting-state connectivity between neurocognitive networks in treatment resistant depression. Front Psychiat 2015;6:28.
de Lacy N, Doherty D, King B, Rachakonda S, Calhoun VD. Disruption to control network function correlates with altered dynamic connectivity in the wider autism spectrum. NeuroImage: Clin 2017;15:513–24.
Demirtaş M, Tornador C, Falcón C, López-Solà M, Hernández-Ribas R, Pujol J, et al. Dynamic functional connectivity reveals altered variability in functional connectivity among patients with major depressive disorder. Hum Brain Mapp 2016;37(8):2918–30.
Díez-Cirarda M, Strafella AP, Kim J, Peña J, Ojeda N, Cabrera-Zubizarreta A, et al. Dynamic functional connectivity in Parkinson's disease patients with mild cognitive impairment and normal cognition. NeuroImage: Clin 2018;17:847–55.
Dong D, Ming Q, Zhong X, Pu W, Zhang X, Jiang Y, et al. State-independent alterations of intrinsic brain network in current and remitted depression. Prog Neuro-Psychopharmacol Biol Psychiat 2019;89:475–80.
Du M-Y, Wu Q-Z, Yue Q, Li J, Liao Y, Kuang W-H, et al. Voxelwise meta-analysis of gray matter reduction in major depressive disorder. Prog Neuro-Psychopharmacol Biol Psychiat 2012;36(1):11–6.
Du Y, Pearlson GD, Yu Q, He H, Lin D, Sui J, et al. Interaction among subsystems within default mode network diminished in schizophrenia patients: a dynamic connectivity approach. Schizophr Res 2016;170(1):55–65.
Dutta A, McKie S, Deakin JW. Resting state networks in major depressive disorder. Psychiat Res: Neuroimag 2014;224(3):139–51.
Ferrari AJ, Charlson FJ, Norman RE, Patten SB, Freedman G, Murray CJ, et al. Burden of depressive disorders by country, sex, age, and year: findings from the global burden of disease study 2010. PLoS Med 2013;10(11):e1001547.
Fox MD, Corbetta M, Snyder AZ, Vincent JL, Raichle ME. Spontaneous neuronal activity distinguishes human dorsal and ventral attention systems. Proc Natl Acad Sci 2006;103(26):10046–51.
Friedman J, Hastie T, Tibshirani R. Sparse inverse covariance estimation with the graphical lasso. Biostatistics 2008;9(3):432–41.
Frodl T, Bokde AL, Scheuerecker J, Lisiecka D, Schoepf V, Hampel H, et al. Functional connectivity bias of the orbitofrontal cortex in drug-free patients with major depression. Biol Psychiat 2010;67(2):161–7.
Gallagher HL, Frith CD. Functional imaging of 'theory of mind'. Trends Cognit Sci 2003;7(2):77–83.
Gazzaley A, Cooney JW, McEvoy K, Knight RT, D'esposito M. Top-down enhancement and suppression of the magnitude and speed of neural activity. J Cognit Neurosci 2005(3):507–17.
Gazzaley A, Cooney JW, Rissman J, D'esposito M. Top-down suppression deficit underlies working memory impairment in normal aging. Nature Neurosci 2005b;8(10):1298.
Gong Q, He Y. Depression, neuroimaging and connectomics: a selective overview. Biol Psychiat 2015;77(3):223–35.
Greicius MD, Flores BH, Menon V, Glover GH, Solvason HB, Kenna H, et al. Resting-state functional connectivity in major depression: abnormally increased contributions from subgenual cingulate cortex and thalamus. Biol Psychiat 2007;62(5):429–37.
Guo W, Liu F, Dai Y, Jiang M, Zhang J, Yu L, et al. Decreased interhemispheric resting-state functional connectivity in first-episode, drug-naive major depressive disorder. Prog Neuro-Psychopharmacol Biol Psychiat 2013a;41:24–9.
Guo W, Liu F, Xue Z, Gao K, Liu Z, Xiao C, et al. Decreased interhemispheric coordination in treatment-resistant depression: a resting-state fMRI study. PLoS One 2013b;8(8):e71368.

Guo Z, Liu X, Li J, Wei F, Hou H, Chen X, et al. Fractional amplitude of low-frequency fluctuations is disrupted in Alzheimer's disease with depression. Clin Neurophysiol 2017;128(7):1344–9.
Gusnard DA, Akbudak E, Shulman GL, Raichle ME. Medial prefrontal cortex and self-referential mental activity: relation to a default mode of brain function. Proc Natl Acad Sci 2001;98(7):4259–64.
Hamilton JP, Chen MC, Gotlib IH. Neural systems approaches to understanding major depressive disorder: an intrinsic functional organization perspective. Neurobiol Dis 2013;52:4–11.
Hamilton JP, Furman DJ, Chang C, Thomason ME, Dennis E, Gotlib IH. Default-mode and task-positive network activity in major depressive disorder: implications for adaptive and maladaptive rumination. Biol Psychiat 2011;70(4):327–33.
Himberg J, Hyvärinen A, Esposito F. Validating the independent components of neuroimaging time series via clustering and visualization. Neuroimage 2004;22(3):1214–22.
Hutchison RM, Womelsdorf T, Allen EA, Bandettini PA, Calhoun VD, Corbetta M, et al. Dynamic functional connectivity: promise, issues, and interpretations. Neuroimage 2013a;80:360–78.
Hutchison RM, Womelsdorf T, Gati JS, Everling S, Menon RS. Resting-state networks show dynamic functional connectivity in awake humans and anesthetized macaques. Hum Brain Mapp 2013b;34(9):2154–77.
Iwabuchi SJ, Peng D, Fang Y, Jiang K, Liddle EB, Liddle PF, et al. Alterations in effective connectivity anchored on the insula in major depressive disorder. Eur Neuropsychopharmacol 2014;24(11):1784–92.
Kaiser RH, Andrews-Hanna JR, Wager TD, Pizzagalli DA. Large-scale network dysfunction in major depressive disorder: a meta-analysis of resting-state functional connectivity. JAMA Psychiat 2015;72(6):603–11.
Kaiser RH, Whitfield-Gabrieli S, Dillon DG, Goer F, Beltzer M, Minkel J, et al. Dynamic resting-state functional connectivity in major depression. Neuropsychopharmacology 2016;41(7):1822.
Kim J, Criaud M, Cho SS, Díez-Cirarda M, Mihaescu A, Coakeley S, et al. Abnormal intrinsic brain functional network dynamics in Parkinson's disease. Brain 2017;140(11):2955–67.
Kober H, Barrett LF, Joseph J, Bliss-Moreau E, Lindquist K, Wager TD. Functional grouping and cortical–subcortical interactions in emotion: a meta-analysis of neuroimaging studies. Neuroimage 2008;42(2):998–1031.
Lehmann D. Brain electric microstates and cognition: the atoms of thought. Machinery of the Mind. Springer; 1990. p. 209–24.
Lemogne C, le Bastard G, Mayberg H, Volle E, Bergouignan L, Lehéricy S, et al. In search of the depressive self: extended medial prefrontal network during self-referential processing in major depression. Social Cognit Affect Neurosci 2009;4(3):305–12.
Li B, Liu L, Friston KJ, Shen H, Wang L, Zeng L-L, et al. A treatment-resistant default mode subnetwork in major depression. Biol Psychiat 2013;74(1):48–54.
Liao W, Zhang Z, Mantini D, Xu Q, Ji G-J, Zhang H, et al. Dynamical intrinsic functional architecture of the brain during absence seizures. Brain Struct Funct 2014;219(6):2001–15.
Liu F, Wang Y, Li M, Wang W, Li R, Zhang Z, et al. Dynamic functional network connectivity in idiopathic generalized epilepsy with generalized tonic–clonic seizure. Hum Brain Mapp 2017;38(2):957–73.
Liu X, Duyn JH. Time-varying functional network information extracted from brief instances of spontaneous brain activity. Proc Natl Acad Sci 2013;110(11):4392–7.
Liu Z, Xu C, Xu Y, Wang Y, Zhao B, Lv Y, et al. Decreased regional homogeneity in insula and cerebellum: a resting-state fMRI study in patients with major depression and subjects at high risk for major depression. Psychiat Res: Neuroimag 2010;182(3):211–5.
Lui S, Wu Q, Qiu L, Yang X, Kuang W, Chan RC, et al. Resting-state functional connectivity in treatment-resistant depression. Am J Psychiat 2011;168(6):642–8.
Ma C, Ding J, Li J, Guo W, Long Z, Liu F, et al. Resting-state functional connectivity bias of middle temporal gyrus and caudate with altered gray matter volume in major depression. PLoS One 2012;7(9):e45263.
Ma Y. Neuropsychological mechanism underlying antidepressant effect: a systematic meta-analysis. Mol Psychiat 2015;20(3):311.
Manoliu A, Meng C, Brandl F, Doll A, Tahmasian M, Scherr M, et al. Insular dysfunction within the salience network is associated with severity of symptoms and aberrant inter-network connectivity in major depressive disorder. Front Hum Neurosci 2014;7:930.
Marusak HA, Calhoun VD, Brown S, Crespo LM, Sala-Hamrick K, Gotlib IH, et al. Dynamic functional connectivity of neurocognitive networks in children. Hum Brain Mapp 2017;38(1):97–108.
Medaglia JD, Lynall M-E, Bassett DS. Cognitive network neuroscience. J Cognit Neurosci 2015;27(8):1471–91.
Menon V. Large-scale brain networks and psychopathology: a unifying triple network model. Trends Cognit Sci 2011;15(10):483–506.
Miller EK, Cohen JD. An integrative theory of prefrontal cortex function. Annu Rev Neurosci 2001;24(1):167–202.
Mulders PC, van Eijndhoven PF, Schene AH, Beckmann CF, Tendolkar I. Resting-state functional connectivity in major depressive disorder: a review. Neurosci Biobehav Rev 2015;56:330–44.
Pascual-Marqui RD, Michel CM, Lehmann D. Segmentation of brain electrical activity into microstates: model estimation and validation. IEEE Trans Biomed Eng 1995;42(7):658–65.
Qin P, Northoff G. How is our self related to midline regions and the default-mode network? Neuroimage 2011;57(3):1221–33.
Rashid B, Damaraju E, Pearlson GD, Calhoun VD. Dynamic connectivity states estimated from resting fMRI Identify differences among Schizophrenia, bipolar disorder, and healthy control subjects. Front Hum Neurosci 2014;8:897.
Rousseeuw PJ. Silhouettes: a graphical aid to the interpretation and validation of cluster analysis. J Comput Appl Math 1987;20:53–65.
Sexton CE, Allan CL, Le Masurier M, McDermott LM, Kalu UG, Herrmann LL, et al. Magnetic resonance imaging in late-life depression: multimodal examination of network disruption. Arch Gen Psychiat 2012;69(7):680–9.
Sheline YI, Barch DM, Price JL, Rundle MM, Vaishnavi SN, Snyder AZ, et al. The default mode network and self-referential processes in depression. Proc Natl Acad Sci 2009;106(6):1942–7.
Shen Y, Yao J, Jiang X, Zhang L, Xu L, Feng R, et al. Sub-hubs of baseline functional brain networks are related to early improvement following two-week pharmacological therapy for major depressive disorder. Hum Brain Mapp 2015;36(8):2915–27.
Stange JP, Bessette KL, Jenkins LM, Peters AT, Feldhaus C, Crane NA, et al. Attenuated intrinsic connectivity within cognitive control network among individuals with remitted depression: temporal stability and association with negative cognitive styles. Hum Brain Mapp 2017;38(6):2939–54.
Tibshirani R, Walther G, Hastie T. Estimating the number of clusters in a data set via the gap statistic. J Roy Stat Soc: Ser B (Stat Methodol) 2001;63(2):411–23.
Van Wingen GA, Tendolkar I, Urner M, van Marle HJ, Denys D, Verkes R-J, et al. Short-term antidepressant administration reduces default mode and task-positive network connectivity in healthy individuals during rest. Neuroimage 2014;88:47–53.
Varoquaux G, Gramfort A, Poline J-B, Thirion B. Brain covariance selection: better individual functional connectivity models using population prior. Adv Neural Informat Process Syst 2010:2334–42.
Vergara VM, Mayer AR, Kiehl KA, Calhoun VD. Dynamic functional network connectivity discriminates mild traumatic brain injury through machine learning. NeuroImage: Clinical 2018;19:30–7.
Wang L-J, Kuang W-H, Xu J-J, Lei D, Yang Y-C. Resting-state brain activation correlates with short-time antidepressant treatment outcome in drug-naive patients with major depressive disorder. J Int Med Res 2014a;42(4):966–75.
Wang L, Li K, Zhang Q, Zeng Y, Dai W, Su Y, et al. Short-term effects of escitalopram on regional brain function in first-episode drug-naive patients with major depressive disorder assessed by resting-state functional magnetic resonance imaging. Psychol Med 2014b;44(7):1417–26.
Wu X, He H, Shi L, Xia Y, Zuang K, Feng Q, et al. Personality traits are related with dynamic functional connectivity in major depression disorder: A resting-state analysis. J Affect Disord 2019;245:1032–42.
Yan C, Zang Y. DPARSF: a MATLAB toolbox for" pipeline" data analysis of resting-state fMRI. Front Syst Neurosci 2010;4:13.
Yao Z, Hu B, Xie Y, Zheng F, Liu G, Chen X, et al. Resting-state time-varying analysis reveals aberrant variations of functional connectivity in autism. Front Hum Neurosci 2016;10:463.
Ye M, Yang T, Qing P, Lei X, Qiu J, Liu G. Changes of functional brain networks in major depressive disorder: a graph theoretical analysis of resting-state fMRI. PLoS One 2015;10(9):e0133775.
Ye T, Peng J, Nie B, Gao J, Liu J, Li Y, et al. Altered functional connectivity of the dorsolateral prefrontal cortex in first-episode patients with major depressive disorder. Eur J Radiol 2012;81(12):4035–40.
Yu Q, Erhardt EB, Sui J, Du Y, He H, Hjelm D, et al. Assessing dynamic brain graphs of time-varying connectivity in fMRI data: application to healthy controls and patients with schizophrenia. Neuroimage 2015;107:345–55.
Zalesky A, Fornito A, Bullmore ET. Network-based statistic: identifying differences in brain networks. Neuroimage 2010;53(4):1197–207.
Zalesky A, Fornito A, Seal ML, Cocchi L, Westin C-F, Bullmore ET, et al. Disrupted axonal fiber connectivity in schizophrenia. Biol Psychiat 2011;69(1):80–9.
Zhang Z, Liu G, Yao Z, Zheng W, Xie Y, Hu T, et al. Changes in dynamics within and between resting-state subnetworks in juvenile myoclonic epilepsy occur at multiple frequency bands. Front Neurol 2018;9.
Zheng H, Li F, Bo Q, Li X, Yao L, Yao Z, et al. The dynamic characteristics of the anterior cingulate cortex in resting-state fMRI of patients with depression. J Affect Disord 2018;227:391–7.
Zheng H, Xu L, Xie F, Guo X, Zhang J, Yao L, et al. The altered triple networks interaction in depression under resting state based on graph theory. Biomed Res Int 2015;2015:386326.
Zhi D, Calhoun VD, Lv L, Ma X, Ke Q, Fu Z, et al. Aberrant dynamic functional network connectivity and graph properties in major depressive disorder. Front Psychiat 2018;9.
Zhu X, Wang X, Xiao J, Liao J, Zhong M, Wang W, et al. Evidence of a dissociation pattern in resting-state default mode network connectivity in first-episode, treatment-naive major depression patients. Biol Psychiat 2012;71(7):611–7.
Zhu X, Zhu Q, Shen H, Liao W, Yuan F. Rumination and default mode network subsystems connectivity in first-episode, drug-naive young patients with major depressive disorder. Sci Rep 2017;7:43105.